A Causal Graph Approach to Oppositional Narrative Analysis

Diego Revilla[1] *, **Martín Fernández-de-Retana**[1] *, **Lingfeng Chen**[1, 2] *,
Aritz Bilbao-Jayo[1, 2] †, **Miguel Fernandez-de-Retana**[1,2] †
[1] Faculty of Engineering, University of Deusto, Bilbao, Spain,
[2]Deusto Institute of Technology, University of Deusto, Bilbao, Spain
Correspondence: m.fernandezderetana@deusto.es, diego.r@opendeusto.es

arXiv:2603.06135v1 [cs.CL] 6 Mar 2026

Abstract

Current methods for textual analysis rely on data annotated within predefined ontologies, often embedding human bias within black-box models. Despite achieving near-perfect performance, these approaches exploit unstructured, linear pattern recognition rather than modeling the structured interactions between entities that naturally emerge in discourse. In this work, we propose a graph-based framework for the detection, analysis, and classification of oppositional narratives and their underlying entities by representing narratives as entity-interaction graphs. Moreover, by incorporating causal estimation at the node level, our approach derives a causal representation of each contribution to the final classification by distilling the constructed sentence graph into a minimal causal subgraph. Building upon this representation, we introduce a classification pipeline that outperforms existing approaches to oppositional thinking classification task.

1 Introduction

Conspiracy theories pose a significant threat to society on multiple levels. They can be deliberately exploited to manipulate public opinion, and exert pressure on public institutions, thereby influencing their decision-making processes (Greenburgh and Raihani, 2022; Moore, 2016). During the COVID-19 pandemic, conspiracy narratives and targeted attacks circulating on social media became a major risk factor which increases the general distrust in institutions (Romer and Jamieson, 2020). Therefore, the automated and fast identification of coordinated narratives and potential aggregated attacks is of critical importance.

The identification of key features that enable the distinction between critical speech and coordinated attacks within a narrative constitutes a complex challenge in natural language processing. This task typically involves uncovering the underlying entities with relational structures in the input text that define the roles participating in such attacks. Moreover, identifying the entities actually involved in such narratives is often challenging due to the subtlety of context and the terms that are normally used with hidden intentions, which complicates the automation of the task, and in many cases, annotators may introduce personal biases or fail to properly resolve references.

Our main contribution lies in extracting a causal graph representation from narrative text and subsequently distilling this graph to identify the primary entities driving a conspiracy narrative. Unlike approaches that depend on labeled data or predefined role schemas, which often introduce edge cases and fail to capture the inherently continuous and diffused nature of participation (Liu and Roth, 2026), our method avoids rigid role assignments. Instead, we enable the model to learn how to select, classify, and filter textual spans in order to construct coherent and contextually appropriate representation of the discourse for classification.

In summary, our main contributions are:

- **Causal Graph Representation:** We propose a pipeline to extract entity-interaction graphs, modeling structural interactions without relying on predefined role schemas.
- **Minimal Causal Graph Distillation:** We introduce a distillation procedure to estimate the Individual Treatment Effect (ITE) of nodes, pruning extraneous nodes and extracting the potential minimal causal subgraph.
- **Graph-Attention Classification Method:** We achieve an F_1-score of 0.93, ranking first in the designated classification task, demonstrating the efficacy of causal graphs for detecting conspiracy vectors.

* These authors contributed equally to this work.
† These authors jointly supervised this work.

In this paper, we train the model to generate a bipartite graph consisting of two sets of vertices. The first set, V, is of dynamic size d and represents the entities identified in the discourse. The second set, E, is a predefined set of size k whose vertices correspond to relation nodes that connect entities. The graph structure is represented by an incidence matrix A.

During the causality stage, we reinterpret this structure as an undirected hypergraph, where the vertices in E are treated as hyperedges over the entity set V. Although this correspondence does not strictly hold in certain edge cases, such as when no relations exist between entities or when the graph is empty, for clarity and simplicity of exposition, we will be treating the *bipartite graph* as an *hypergraph* throughout this work.

Table 4 (Appendix) summarizes all hyperparameters and equipment used in the experimental setup. The implementation of the model and the source code to replicate the experiment can be found at Github Repository

2 Related Work

Entity Framing: The original task named entity recognition has been approached in various ways. Before the emergence of deep learning (Rumelhart et al., 1986) and other black-box models, Natural Policy Framing (Blair and McCormack, 2016) was proposed as a methodological approach based on content analysis to identify the classic narrative roles of hero, villain, and victim. This framework was later refined with approaches that leveraged role dictionaries and sentiment analysis (Gomez-Zara et al., 2018).

The task was then generalized to entity framing, which combines two sub-tasks: identifying characters and classifying the roles assigned to each character. In the present, the predominating technique in the state of the art consist of fine-tuning a foundational LLM for the specific NER task (Mahmoud et al., 2025).

Inherent Graph Representation: Many problems and real-world scenarios can be naturally represented as graphs, such as RNA structure prediction (Koessler et al., 2010) and Protein-Protein Interaction (Xu et al., 2024). This structural perspective has motivated the development of Graph Neural Networks (GNNs) (Scarselli et al., 2009). However, certain tasks require the explicit modeling of causal relationships within the underlying context, thereby motivating the integration of causal inference principles into graph-based methods. This line of work has given rise to Causal Graph Neural Networks (Causal GNNs) (Wein et al., 2020; Du et al., 2024).

Subsequently, causal discovery methods were further enhanced through GNN-based probabilistic frameworks that learn stochastic distributions over the space of possible graph structures (Rashid and Terejanu, 2024). Moreover, recent efforts have focused on learning robust graphical representations and performing neural architecture search in real-world settings where the i.i.d. assumption does not hold, such as in datasets exhibiting distribution shifts (Wang et al., 2025; Li et al., 2024a).

In the field of natural language processing, several efforts have been made to transform human-readable text into graph-based representations. The main goal is to improve the performance of current state-of-the-art models on tasks such as text classification, where subcontextual information can be captured more effectively in graphs (Bugueño and de Melo, 2023). Within this line of research, linguistic approaches use large language models (LLMs) to summarize information and convert it into nodes, which are then connected through semantic relationships (Li et al., 2025). Graph-based text classification can also be improved with contrastive learning and data augmentation, where augmented graphs are generated from the text to improve generalization performance (Li et al., 2024b). Furthermore, unsupervised methods based on cyclic training have been proposed, especially for smaller datasets, where the high cost of data collection makes fully supervised learning less feasible (Guo et al., 2020).

Graph Interpretation Problem: Evaluating and interpreting graphical representations of real-world information to determine their quality, as well as assessing the extent of information preserved or lost, remains a challenging task. Focusing on the evaluation of a graphical representation, HL-HGAT (Hodge-Laplacian Heterogeneous Graph Attention Network) (Huang et al., 2024), a graphical neural network that extends GNNs to handle not only nodes and edges, but also higher-dimensional simplices (e.g., triangles). In terms of interpretability and explainability, several traditional techniques were adapted to graph representations. FactGraph is a framework that evaluates the factual consistency of a graph representation of a summary (or text) with respect to the source document (Ribeiro

et al., 2022).

From the perspective of explainability, several adaptations of classical machine learning approaches to graphs have been presented in recent years, such as gradient-based methods and counterfactual explanations (Nandan et al., 2025). CF-GNNExplainer is a counterfactual explanation method based on distortion matrices, which generates perturbations in the input graph to produce counterfactual examples that reveal how the graph structure influences the model's behavior (Lucic et al., 2022).

3 Methodology

Our approach is inspired by SpERT (Markus and Adrian, 2020), which proposes an iterative algorithm for joint entity extraction and classification with a strong reliance on accurately labeled entity spans. While SpERT demonstrates strong performance, it depends heavily on high-quality annotations.

Our proposal extends this paradigm by improving the detection task and incorporating causal modules that allow for a structured interpretation of the model's predictions. In particular, we aim not only to enhance entity and relation identification, but also to provide insight into the underlying decision-making process, thereby increasing the transparency and interpretability of the overall framework.

One measure taken to improve the performance of the BERT (Devlin et al., 2019) model within the framework was to fine-tune it on the LOCO dataset (Miani et al., 2021) for a classification task. After this stage, the model was kept frozen and applied to the target dataset of oppositional narratives for the same task.

Each stage of the proposed methodology is presented and graphically illustrated in Figure 1.

Span Extraction & Entity Classification

We assume that if a span belongs to a given category, then all of its subspans also belong to the same category. However, the converse does not necessarily hold: if a span does not belong to a category, this does not imply that its subspans are excluded from that category. For example, if *"President Obama"* is annotated as an entity, then *"President"* is also considered an entity in the corresponded discourse under this assumption. In contrast, a longer span such as *"The President Obama from the White House"* may not be annotated as an entity, even though it contains a valid entity as a subspan.

Based on this assumption, we propose a span-framing procedure to extract all possible entity candidates from the input narrative (see Algorithm 1 in Appendix A). The algorithm enumerates spans greedily up to a maximum width of w_{max}. Each candidate span of width k starting at position i is represented by concatenating three vectors: the sentence-level `[CLS]` embedding, the component-wise maximum pooling of the k constituent embeddings, and a learned span-width embedding. This representation is passed to a linear span classifier that assigns one of N predefined, fixed entity types or a null *no-span* class.

Entity Projection & Enrichment

Once all entities are extracted, each entity is linearly projected into a lower-dimensional embedding space, as it has been proven to alleviate overfitting. These projected embeddings are then jointly enriched using a lightweight Transformer encoder, which models contextual interactions among all extracted entities.

Bipartite Graph Construction

For each entity (corresponding to a vertex in V), a multilayer perceptron produces a binary adjacency vector indicating its connections to vertices in E, which represent relational factors or correlation nodes between entities. Discrete relation membership is obtained via a Gumbel-Sigmoid estimator (Jang et al., 2017) and hard thresholding, enabling end-to-end training through the discrete selection. This process results in the construction of a bipartite graph for the given input text.

HGT Classification

To enable the model to learn meaningful graph-based representations of the narrative text, we employ a Heterogeneous Graph Transformer (HGT) (Hu et al., 2020) for graph-level classification.

HGT is particularly suitable for modeling narrative graphs containing correlated entities and coordinated interactions, as it explicitly accounts for structural and semantic heterogeneity through and class-aware relational attention. By assigning node and edge-type dependent projection matrices, HGT captures role-specific influence patterns and interaction asymmetries while maintaining parameter

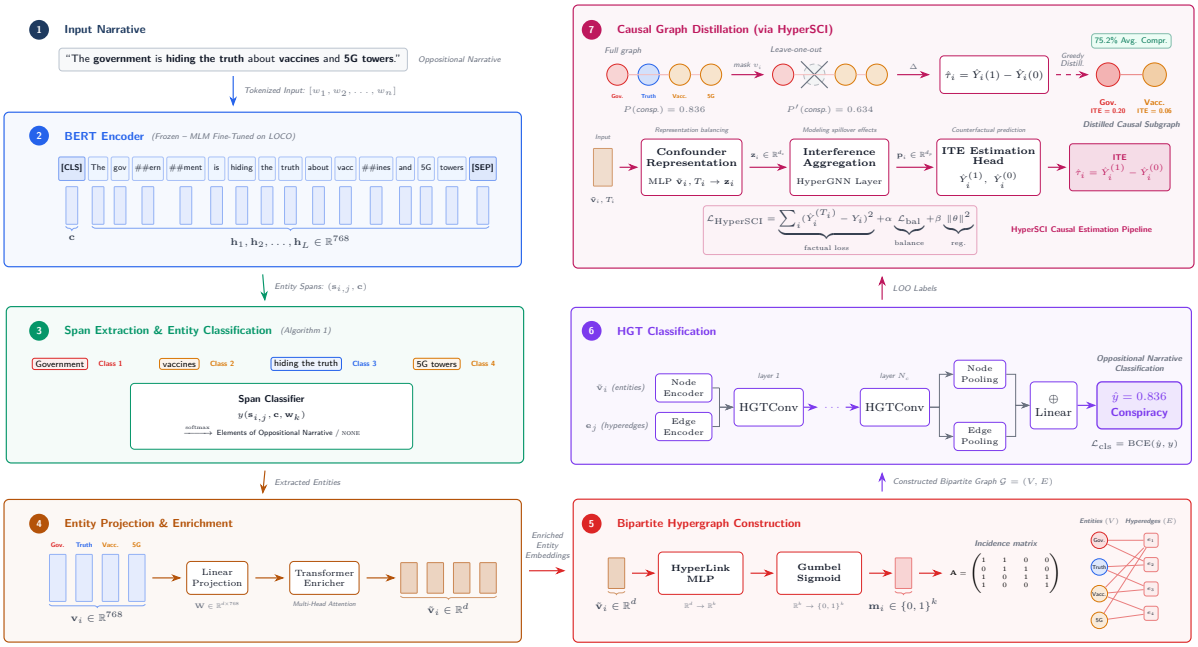

Figure 1: Overview of the proposed methodology. Stage 1 defines the input, which in this case consists of oppositional narratives. Stage 2 generates tokens and contextual embeddings using BERT. Stage 3 extracts the entities V from the tokens and embeddings applying the Algorithm 1 (Appendix). Stage 4 produces enriched low-dimensional representations of the entities. Stage 5 constructs the adjacency matrix A. Stage 6 performs graph classification. Finally, the last stage presents the causal analysis.

sharing for efficient generalization. These properties make HGT especially effective for identifying implicit relational motifs, modeling higher-order dependencies, and detecting orchestrated or aggregated attacks in complex narrative graphs.

The HGT operates over the constructed bipartite graph and is trained under supervision at the narrative level. Specifically, each graph corresponding to a full text is assigned a global label (e.g., *critical* or *conspiracy*), and the model is optimized to predict this label, thereby learning graph representations that capture the structural discriminative patterns for narrative classification.

Through this supervision signal, the model adjusts its weights to learn entity and relational representations that discriminate between critical and conspiracy narratives. In this way, the graph encoder is encouraged to highlight the structural and semantic patterns that characterize each narrative type.

Although the overall architecture is complex, the vast majority of the model parameters are concentrated in the text encoder (BERT). In contrast, the graph construction and reasoning components introduce only a relatively small overhead: fewer than 200K additional parameters are required to build the bipartite graph from token embeddings and to model the corresponding conspiracy narrative structure. A detailed parameter breakdown is provided in Table 1.

Components	Parameters	Percentage (%)
BERT (frozen)	109,483,778	99.841
Enricher	2,240	0.002
HyperLink Classifier	759	0.001
Hyper-Graph Classifier	126,745	0.116
Entity Projector	24,592	0.022
Span Classifier	11,525	0.011
Width Embeddings	4,608	0.004
Type Embeddings	3,840	0.004
Total	**109,658,087**	**100.00**

Table 1: Decomposition of the total number of model parameters by component.

Causal Graph Distillation

To study the causality of each of the graphs in our model, we chose to implement the HyperSCI model (Ma et al., 2022), designed to estimate the Individual Treatment Effect (ITE) as a correlation indicator (Zhang and Richardson, 2025) where the causal relationship is not independent, taking into account the interaction between nodes through hyper-edges. As discussed in an earlier section, the adjacency matrix of the generated bipartite graph can also be

used to construct a hypergraph representation.

Confounder Representation Learning

In observational studies, a confounder (Jager et al., 2008) is defined as a correlation that is not causal but is observable in the dataset. To mitigate this, HyperSCI uses an MLP to project the characteristics of the nodes X into a space where all potential confounders are expected to be found, thus enabling the model to control these effects in the latent space Z. To ensure that the distribution of confounders in Z is invariant after projection into the represented space, a regularization technique based on the Wasserstein distance (Chewi et al., 2025) is implemented, minimizing the out-of-distribution variance between the distributions of the treatment nodes and the control nodes:

$$\mathcal{L}_{was} = \text{Wasserstein}(Z_{treatment}, Z_{control})$$

Inference Modelling

The interference module propagates representations of confounders Z through the hypergraph $\mathcal{G}$. For a node i, the interference representation P_i aggregates (spillover) information from its neighbors:

$$H^{(l+1)} = \sigma(\text{HyperGNN}(H^{(l)}, \mathcal{G}, T))$$

Where T acts as a weight in the propagation, allowing the model to understand how the presence/absence of neighboring entities alters the causal context of node i. This allows us to estimate the ITE under spillover effects (propagation of information to neighboring nodes).

ITE Prediction

Finally, we concatenate the representation of confusers z_i and the representation of interference Pi, where our end heads will give us two outputs: $\hat{Y}(1)$, prediction of the output if the node is present, and $\hat{Y}(0)$, prediction of the output if the node is NOT present. We calculate the ITE as:

$$\hat{\tau}_i = \hat{Y}_i(1) - \hat{Y}_i(0)$$

Leave-One-Out

Since we lack actual counterfactual causal labels, we construct a synthetic dataset using Leave-One-Out (LOO). For each text d in the training set, we define

$$Y_i(t) = P\big(\text{conspiracy} \mid \mathcal{G}_{d\setminus(1-t)\{i\}}\big)\,, t \in \{0, 1\}$$

where $\mathcal{G}_d$ is the complete hypergraph of document d, and $\mathcal{G}_{d\setminus\{i\}}$ denotes the hypergraph with the characteristics of node i set to zero. Note that $Y_i(1)$ is identical for all nodes in the same document (base probability), while $Y_i(0)$ is specific to each node. The ITE$_{true}$ is defined as:

$$\begin{aligned}\tau_i &= Y_i(1) - Y_i(0) \\ &= P(\text{conspiracy} \mid \mathcal{G}_d) - P\big(\text{conspiracy} \mid \mathcal{G}_{d\setminus\{i\}}\big)\end{aligned}$$

The final objective function combines the mean squared error (MSE) with a regularization term:

$$\mathcal{L} = \sum_i \left(\hat{y}_{i,\text{factual}} - y_{i,\text{true}}\right)^2 + \alpha \cdot \mathcal{L}_{was} \qquad (1)$$

where $y_{i,\text{true}}$ denotes the observed factual outcome, $\hat{y}_{i,\text{factual}}$ represents the prediction produced by the HyperSCI model for the factual instance, and α is a hyperparameter that controls the contribution of the Wasserstein regularization term $\mathcal{L}_{was}$.

Once the ITEs for each node have been obtained, we obtain the causal nodes by sorting the nodes with the highest ITE and unmasking them from the graph until the model makes a prediction contrary to the original one, in a greedy search style.

Spillover Mitigation

Due to BERT's attention mechanism, information about an entity tends to be distributed among the attended tokens. If the encoder is trained dynamically alongside the causal model, it could learn to "hide" entity information in the neighboring context to maximize classification performance (Vaswani et al., 2017; He et al., 2021), thereby invalidating the semantic information of each token and causing a uniform ITE for each node in the graph. To mitigate this risk and ensure that entity embeddings are faithful to their intrinsic semantic meaning, we implement an alternative strategy for the causal task:

1. Domain-Adaptive Pre-training (Masked Language Modeling): Before constructing the hypergraph, we subject the base model (BERT) to an unsupervised fine-tuning process on the domain-specific corpus using the Masked Language Modeling (MLM) task. This specializes the encoder to generate discriminative and semantically rich vector representations for entities in the conspiracy domain, improving separability in the latent space.

2. During the training phase of the HyperSCI causal model, we freeze the weights of the pre-trained BERT encoder, preventing the encoder from adapting to compensate for node masking and favoring final classification over individual causality.

4 Results

4.1 Dataset

We test the proposed architecture with the dataset from PAN 2024 Oppositional Narratives (Korenčić et al., 2024)

The dataset used in this work is based on the XAI-DisInfodemic corpus (Korenčić et al., 2024), which consists of 10,000 Telegram messages, 5,000 in English and 5,000 in Spanish, containing dissenting and non-conventional opinions about the COVID-19 pandemic. These messages are divided into two categories: those suggesting the existence of a conspiracy, and those that criticize mainstream views on the COVID-19 pandemic without implying the existence of a conspiracy.

Focusing on the official English subset, the training split contains 4,000 samples, encompassing 1,379 conspiratorial and 2,621 critical texts. This class distribution is closely mirrored in the 1,000 sample test set, which consists of 345 conspiratorial and 655 critical instances, ensuring consistent class proportions across the evaluation phases.

Language	Avg.	Std. dev	Min.	Q1	Median	Q3	Max.
Spanish	128	123	23	49	98	148	766
English	265	528	12	32	65	266	4 108

Table 2: Text length statistics measured in number of words (Korenčić et al., 2024).

A key limitation of this dataset is its relatively small size for training classification tasks. To mitigate this issue, we make use of the LOCO (Language Of Conspiracy) dataset (Miani et al., 2022), which is an 88-million-token, open-source corpus featuring 23,937 conspiracy and 72,806 topic-matched mainstream documents from 150 websites. To mitigate this concern, the BERT model was fine-tuned on the LOCO corpus and then frozen for text classification. This corpus is considerably larger than the one used in the present work, allowing access to linguistic representations already adapted to the domain.

Team	MCC$^{\uparrow}$	F_1-Macro$^{\uparrow}$	F_1-Cons.$^{\uparrow}$	F_1-Crit.$^{\uparrow}$
Our Model	**0.840**	**0.920**	**0.895**	**0.945**
IUCL	0.838	0.919	0.894	0.944
AI_Fusion	0.830	0.914	0.886	0.942
SINAI	0.829	0.914	0.888	0.941
ezio	0.821	0.909	0.879	0.940
Baseline-BERT	0.796	0.897	0.863	0.931

Table 3: Classification results of our model compared to the PAN 2024 benchmark (Korenčić et al., 2024). Our model outperforms IUCL (Mhalgi et al., 2024), AI_Fusion, and SINAI (Vallecillo-Rodríguez et al., 2024).

4.2 Classification Performance

The proposed system achieves a macro F_1-score of 0.93, thus only misclassifying 72 samples out of the 1000 in the English test set. Furthermore, when compared to the official task results presented in Table 3, our model ranks first overall with a Matthews Correlation Coefficient (MCC) of 0.8407. Notably, our approach is also highly parameter-efficient. As detailed in the parameter breakdown in Table 1 , the proposed architecture operates with approximately 109M parameters, roughly one-third of the parameter count of the second place solution, which relies on a heavier DeBERTa-large model (304M parameters).

4.3 Causal Inference and Explainability

We evaluate the causal effect using two criteria: the Precision in Estimation of Heterogeneous Effect (PEHE) (Hill, 2011), which reflects how accurately the model estimates each treatment effects, and the Average Treatment Effect (ATE), which captures the mean impact of the treatment on the outcome.

Our model achieves a PEHE of 0.2994 and an ATE of 0.0218. These results indicate that the general causal estimation error remains non-negligible, while the relatively low ATE suggests that the average causal differences across individual units are modest.

While the current architecture successfully captures several of the most critical causal relationships, the initial metrics highlight exciting avenues for future optimization. In particular, the model final PEHE suggests an opportunity to improve the accuracy of our individual causal predictions. Additionally, ATE indicates that rather than being highly concentrated, the distribution of causal impact across nodes is extremely delicate and granular. Due to these metrics, we can conclude that it serves as a proof-of-concept with room for improvement.

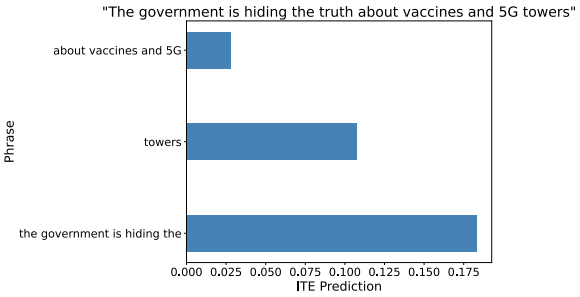

Figure 2: An oppositional narrative text correctly classified as Conspiracy, with a predicted probability of 0.836, indicating high model confidence.

To analyze interpretability, Individual Treatment Effects (ITEs) were computed for selected text examples. An example is illustrated in Figure 2.

4.4 Minimal Subgraph Compression

To identify the minimal causal subgraph, we quantified the extent to which the entity graph can be compressed while preserving correct predictions. The *compression rate* (CR) is defined as:

$$\text{CR} = \left(1 - \frac{|V_{\text{remaining}}|}{|V|}\right) \times 100$$

On average, the model requires only a small fraction of entities to make a correct decision, suggesting effective causal attribution. In the future, it should be tested with a larger number of classes to more extensively test the need for graphs, as currently 67% of classes can be guessed without any nodes (which corresponds to the number of non-conspiratorial classes, which is the majority class). Because the final classification head utilizes a sigmoid activation, in the absence of graph-based structural signals (i.e., a fully compressed graph), the model naturally outputs its learned bias.

Further insights into the model's causal attribution can be observed through the analysis of minimal subgraph compression rates. The system achieves an overall average compression rate of 75.2% , a standard deviation of $\sigma = 7.8$, and a maximum of 96.2%. When analyzing the performance by category, the mean compression rate is 72.8% for critical texts and 79.6% for conspiratorial texts. These figures demonstrate that the model is capable of formulating accurate predictions relying on only a small fraction of the entities present in the causal graph.

5 Ablations

A modification has been made to the causal inference process, consisting of removing the enrichment module from the causal inference model with BERT fine-tuned for MLM. This change has a considerable impact on system performance, causing a decrease in the F_1 score from approximately 0.93 to 0.86.

6 Conclusion

This work presents a novel modular architecture based on a causal entity framing graph to effectively distinguish between critical narratives and conspiracy theories. By leveraging intermediate graph representations, our proposed framework successfully applies causal inference techniques to uncover the true underlying drivers of the model's classification decisions. The proposed methodology demonstrates state-of-the-art efficacy, achieving an F_1-score of 0.93 and ranking first in the designated task and based on the following principles:

Domain Adaptation: Pre-training the model on the extensive LOCO dataset significantly improved its capacity to generalize, overcoming the limitations of the much smaller task-specific dataset.

Relationship Representation: Structuring entity relationships as graphs provided a superior method for representing the complex semantic information contained within the text.

Causal Inference: Utilizing these intermediate graph structures allowed for a highly interpretable view into the model's decision-making process.

7 Future Work

We identify two primary points for future research to enhance the proposed framework. First, sophisticated methods are required to mitigate spillover effects, aiming to develop a more accurate and representative causal description. Finally, exploring alternative approaches for the Entity Framing phase, such as Deep SpERT (Zhu et al., 2023), could potentially lead to superior results during the initial entity extraction pipeline.

8 Limitations

Although our architecture achieves state-of-the-art performance, ranking first in the PAN 2024 oppositional thinking classification task, its cross-dataset generalization remains unverified. However, we

solved local data scarcity through domain-adaptive pretraining on the larger LOCO corpus but have not yet been able to test how robust our framework is to various linguistic sources since there is currently very little available data with comprehensive annotations for highly specialized areas such as oppositional and conspiracy narratives. Besides, the synthetic nature of LOO labels provides an approximation based on predictive importance rather than a ground-truth ITE. As a result, the causal model may struggle to learn deeper, interleaved correlations and reflects the influence of each node on the classifier's output.

9 Ethical Considerations

The capability to detect coordinated narratives can cut both ways. It can help identify and prevent disinformation campaigns targeting public health or coordinated attacks against democratic institutions. Nonetheless it may also be misused as an automated censorship tool to detect so-called "undesired" speech, enabling the identification and suppression of political opponents.

10 Acknowledgments

We gratefully acknowledge the support of the Ministry of Economy, Industry, and Competitiveness of Spain under Grant No.:INCEPTION (PID2021-128969OB-I00) and the Basque Government under the grant DEUSTEK5 (IT1582-22).

References

Benjamin D Blair and Larkin McCormack. 2016. Applying the narrative policy framework to the issues surrounding hydraulic fracturing within the news media: A research note. *Research & Politics*, 3(1):2053168016628334.

Margarita Bugueño and Gerard de Melo. 2023. Connecting the dots: What graph-based text representations work best for text classification using graph neural networks? In *Findings of the Association for Computational Linguistics: EMNLP 2023*, page 8943–8960. Association for Computational Linguistics.

Sinho Chewi, Jonathan Niles-Weed, and Philippe Rigollet. 2025. *Estimation of Wasserstein Distances*, pages 37–76. Springer Nature Switzerland, Cham.

Jacob Devlin, Ming-Wei Chang, Kenton Lee, and Kristina Toutanova. 2019. Bert: Pre-training of deep bidirectional transformers for language understanding. *Preprint*, arXiv:1810.04805.

Xiaojing Du, Feiyu Yang, Wentao Gao, and Xiongren Chen. 2024. Causal gnns: A gnn-driven instrumental variable approach for causal inference in networks. *Preprint*, arXiv:2409.08544.

Diego Gomez-Zara, Miriam Boon, and Larry Birnbaum. 2018. Who is the hero, the villain, and the victim? detection of roles in news articles using natural language techniques. In *Proceedings of the 23rd International Conference on Intelligent User Interfaces*, IUI '18, page 311–315, New York, NY, USA. Association for Computing Machinery.

Anna Greenburgh and Nichola J. Raihani. 2022. Paranoia and conspiracy thinking. *Current Opinion in Psychology*, 47:101362.

Qipeng Guo, Zhijing Jin, Xipeng Qiu, Weinan Zhang, David Wipf, and Zheng Zhang. 2020. Cyclegt: Unsupervised graph-to-text and text-to-graph generation via cycle training. *Preprint*, arXiv:2006.04702.

Pengcheng He, Xiaodong Liu, Jianfeng Gao, and Weizhu Chen. 2021. Deberta: Decoding-enhanced bert with disentangled attention. In *International Conference on Learning Representations*.

Jennifer L. Hill. 2011. Bayesian nonparametric modeling for causal inference. *Journal of Computational and Graphical Statistics*, 20(1):217–240.

Ziniu Hu, Yuxiao Dong, Kuansan Wang, and Yizhou Sun. 2020. Heterogeneous graph transformer. *Preprint*, arXiv:2003.01332.

Jinghan Huang, Qiufeng Chen, Yijun Bian, Pengli Zhu, Nanguang Chen, Moo K. Chung, and Anqi Qiu. 2024. Advancing graph neural networks with hl-hgat: A hodge-laplacian and attention mechanism approach for heterogeneous graph-structured data. *Preprint*, arXiv:2403.06687.

K.J. Jager, C. Zoccali, A. MacLeod, and F.W. Dekker. 2008. Confounding: What it is and how to deal with it. *Kidney International*, 73(3):256–260.

Eric Jang, Shixiang Gu, and Ben Poole. 2017. Categorical reparameterization with gumbel-softmax. In *International Conference on Learning Representations*.

Denise R. Koessler, Debra J. Knisley, Jeff Knisley, and Teresa Haynes. 2010. A predictive model for secondary rna structure using graph theory and a neural network. *BMC Bioinformatics*, 11(6):S21.

Damir Korenčić, Berta Chulvi, X Bonet Casals, Mariona Taulé, Paolo Rosso, and Francisco Rangel. 2024. Overview of the oppositional thinking analysis pan task at clef 2024. *Working Notes of CLEF*.

Damir Korenčić, Berta Chulvi, Xavier Bonet Casals, Alejandro Toselli, Mariona Taulé, and Paolo Rosso. 2024. What distinguishes conspiracy from critical narratives? a computational analysis of oppositional discourse. *Expert Systems*, 41(11).

Peiwen Li, Xin Wang, Zeyang Zhang, Yijian Qin, Ziwei Zhang, Jialong Wang, Yang Li, and Wenwu Zhu. 2024a. Causal-aware graph neural architecture search under distribution shifts. *Preprint*, arXiv:2405.16489.

Ximing Li, Bing Wang, Yang Wang, and Meng Wang. 2024b. Graph-based text classification by contrastive learning with text-level graph augmentation. *ACM Trans. Knowl. Discov. Data*, 18(4).

Zehan Li, Ruhua Pan, and Xinyu Pi. 2025. Beyond llms: A linguistic approach to causal graph generation from narrative texts. *Preprint*, arXiv:2504.07459.

Siyi Liu and Dan Roth. 2026. Conflicts in texts: Data, implications and challenges. *Preprint*, arXiv:2504.19472.

Ana Lucic, Maartje A. Ter Hoeve, Gabriele Tolomei, Maarten De Rijke, and Fabrizio Silvestri. 2022. Cf-gnnexplainer: Counterfactual explanations for graph neural networks. In *Proceedings of The 25th International Conference on Artificial Intelligence and Statistics*, volume 151 of *Proceedings of Machine Learning Research*, pages 4499–4511. PMLR.

Jing Ma, Mengting Wan, Longqi Yang, Jundong Li, Brent Hecht, and Jaime Teevan. 2022. Learning causal effects on hypergraphs. In *Proceedings of the 28th ACM SIGKDD Conference on Knowledge Discovery and Data Mining*, KDD '22, page 1202–1212, New York, NY, USA. Association for Computing Machinery.

Tarek Mahmoud, Zhuohan Xie, Dimitar Dimitrov, Nikolaos Nikolaidis, Purificação Silvano, Roman Yangarber, Shivam Sharma, Elisa Sartori, Nicolas Stefanovitch, Giovanni Da San Martino, Jakub Piskorski, and Preslav Nakov. 2025. Entity framing and role portrayal in the news. *Preprint*, arXiv:2502.14718.

Eberts Markus and Ulges Adrian. 2020. Span-based joint entity and relation extraction with transformer pre-training. In *ECAI 2020*. IOS Press.

Shrirang Mhalgi, Srikar Kashyap Pulipaka, and Sandra Kübler. 2024. Iucl at pan 2024: Using data augmentation for conspiracy theory detection. In *CLEF (Working Notes)*, pages 2797–2806.

Alessandro Miani, Thomas Hills, and Adrian Bangerter. 2021. LOCO: The 88-million-word language of conspiracy corpus. *Behav Res Methods*, 54(4):1794–1817.

Alessandro Miani, Thomas Hills, and Adrian Bangerter. 2022. Loco: The 88-million-word language of conspiracy corpus. *Behavior Research Methods*, 54(4):1794–1817.

Alfred Moore. 2016. Conspiracy and conspiracy theories in democratic politics. *Critical Review*, 28(1):1–23.

Mauparna Nandan, Soma Mitra, and Debashis De. 2025. Graphxai: a survey of graph neural networks (gnns) for explainable ai (xai). *Neural Computing and Applications*, 37(17):10949–11000.

Rezaur Rashid and Gabriel Terejanu. 2024. Graph neural networks for probabilistic causal discovery. In *9th Causal Inference Workshop at UAI 2024*.

Leonardo F. R. Ribeiro, Mengwen Liu, Iryna Gurevych, Markus Dreyer, and Mohit Bansal. 2022. Factgraph: Evaluating factuality in summarization with semantic graph representations. *Preprint*, arXiv:2204.06508.

Daniel Romer and Kathleen Hall Jamieson. 2020. Conspiracy theories as barriers to controlling the spread of covid-19 in the u.s. *Social Science & Medicine*, 263:113356.

David E. Rumelhart, Geoffrey E. Hinton, and Ronald J. Williams. 1986. Learning representations by back-propagating errors. *Nature*, 323(6088):533–536.

Franco Scarselli, Marco Gori, Ah Chung Tsoi, Markus Hagenbuchner, and Gabriele Monfardini. 2009. The graph neural network model. *IEEE Transactions on Neural Networks*, 20(1):61–80.

María Estrella Vallecillo-Rodríguez, María Teresa Martín-Valdivia, and Arturo Montejo-Ráez. 2024. Sinai at pan 2024 oppositional thinking analysis: Exploring the fine-tuning performance of large language models.

Ashish Vaswani, Noam Shazeer, Niki Parmar, Jakob Uszkoreit, Llion Jones, Aidan N Gomez, Ł ukasz Kaiser, and Illia Polosukhin. 2017. Attention is all you need. In *Advances in Neural Information Processing Systems*, volume 30. Curran Associates, Inc.

Yuhan Wang, Silu He, Qinyao Luo, Hongyuan Yuan, Ling Zhao, Jiawei Zhu, and Haifeng Li. 2025. Causal invariant geographic network representations with feature and structural distribution shifts. *Future Generation Computer Systems*, 169:107814.

Simon Wein, Wilhelm Malloni, Ana Maria Tomé, Sebastian M. Frank, Gina-Isabelle Henze, Stefan Wüst, Mark W. Greenlee, and Elmar W. Lang. 2020. A graph neural network framework for causal inference in brain networks. *Preprint*, arXiv:2010.07143.

Mingda Xu, Peisheng Qian, Ziyuan Zhao, Zeng Zeng, Jianguo Chen, Weide Liu, and Xulei Yang. 2024. Graph neural networks for protein-protein interactions – a short survey. *Preprint*, arXiv:2404.10450.

Zhehao Zhang and Thomas S. Richardson. 2025. Individual treatment effect: Prediction intervals and sharp bounds. *Preprint*, arXiv:2506.07469.

Enwei Zhu, Yiyang Liu, and Jinpeng Li. 2023. Deep span representations for named entity recognition. *Preprint*, arXiv:2210.04182.

A Appendix

The following pseudocode 1 describes the algorithm we designed to extract entities from token representations using contextual embeddings and a max-pooling aggregation strategy. The algorithm is formulated under the assumptions stated in the main text of this article.

To ensure computational tractability, the algorithm constrains the maximum allowable length of each candidate span. This restriction reduces the space of all possible candidates to a manageable and computationally feasible set.

Parameter	**Value**
Span & Entity Representation	
max_span_width	5
num_span_type	4
entity_dim	16
dropout_rate	0.15
Hyperlink Module	
num_hyperlink	7
hyperlink_features_dim	16
hyper_link_classifier_hidden_dim	[]
hyper_link_classifier_activation	ELU
gumbel_sigmoid_tau	$0.5 \rightarrow 0$
gumbel_sigmoid_hard	True
Enricher (Transformer)	
enricher_n_heads	4
enricher_num_layers	1
enricher_dim_feedforward	32
enricher_use_cls	True
enricher_max_len	200
enricher_padding_value	0.0
Hypergraph Backbone	
hyper_graph_feature_extractor	HGT
hyper_graph_hidden_dim	64
hyper_graph_out_dim	64
hyper_graph_heads	4
hyper_graph_dropout	0.15
hgt_num_layers	2
num_outputs	1
Training Setup	
Optimizer	AdamW
Weight decay	10^{-5}
Learning rate	10^{-4}
Batch size	500
Epochs	10

Table 4: Hyperparameters of the experiment

Table 4 includes the set of hyperparameters used for the experiments. Take note that the hyperparameter num_hyperlink refers to the set size k and all the hyperlink references are the set E.

Algorithm 1 Bipartite Graph Vertex Selection

Require: Embedding sequence $T = (h_0, \ldots, h_{L-1})$ of length L, where h_0 corresponds to `[CLS]` and some h_ℓ corresponds to `[SEP]`; maximum span size K; p embedding projection function; and y span classification function.

Ensure: Matrix $E \in \mathbb{R}^{N \times d}$ containing the embeddings of the hypergraph vertices.

$c \leftarrow T[0]$
$i \leftarrow 1$
$k \leftarrow K$
$E \leftarrow [\,]$ {(empty) list of selected embeddings}
while $k \geq 1$ **do**
  if $i = L$ **then**
    return E
  end if
  $w \leftarrow W(k)$
  $s \leftarrow T[i : i + k]$
  if $y(s, c, w) \notin \{\text{NONE}\}$ **then**
    add $p(s, c)$ to E
    if $L - (i + k) < k$ **then**
      $k \leftarrow L - (i + k)$
      $i \leftarrow L - k$
    else if $|E| = 0 \wedge K > 1$ **then**
      $k \leftarrow k - 1$
      $i \leftarrow 0$
    else
      $i \leftarrow i + k$
    end if
  else
    if $i + k \geq L$ **then**
      $k \leftarrow L - (i + 1)$
    else
      $i \leftarrow i + 1$
    end if
  end if
end while
return E